J. Fluid Mech. (2010), *vol.* 649, *pp.* 19–43.
doi:10.1017/S0022112009993351

Water bells formed on the underside of a horizontal plate. Part 1. Experimental investigation

GRAEME J. JAMESON[1]†, CLAIRE E. JENKINS[1], ELEANOR C. BUTTON[2] AND JOHN E. SADER[2]

[1]Centre for Multiphase Processes, University of Newcastle, Callaghan, New South Wales 2308, Australia

[2]Department of Mathematics and Statistics, University of Melbourne, Victoria 3010, Australia

(Received 6 November 2008; revised 9 November 2009; accepted 9 November 2009)

In this study we report discovery of a new type of water bell. This is formed by impinging a vertical liquid jet on to the underside of a large horizontal flat plate. After impact, the liquid spreads radially along the plate before falling at an abrupt unspecified radius. This falling liquid may then coalesce to form a curtain which encloses a volume of air. When the flow rate of the impinging jet is altered from the value at initial formation, a pronounced hysteretic effect in the water bell shape can be observed. We present detailed observations of these new phenomena, including the size and nature of the flow underneath the plate and the shape of the liquid curtain. These observations are interpreted theoretically in a companion paper (Part 2, Button *et al.* vol. 649, 2010, pp. 45–68).

1. Introduction

When a liquid jet impacts a small disk or cone, a free moving liquid sheet is created. If this sheet closes, trapping a mass of air, it is known as a 'water bell'. These water bells have continued to attract attention since their discovery, by Felix Savart, in 1833. Typically, a vertical liquid jet is aimed down, and impacts a disk perpendicular to the direction of flow. Examples of these classical water bells can be seen in Taylor (1959*a*) and Clanet (2001). Several other experimental arrangements have been used to create water bells. For example, Hopwood (1952) and Brunet, Clanet & Limat (2004) constructed an overflowing tube and dish respectively as a means for generating a liquid sheet. However they are produced, water bells possess a great beauty. Many studies have investigated the shape and stability of the various water bells, since in addition to their aesthetic quality, liquid bells, sheets and their stability have numerous applications. The liquid sheet falling under gravity is used in many coating processes (Finnicum, Weinstein & Ruschak 1993) and paper manufacturing (Söderberg & Alfredsson 1998). Disintegration of a liquid curtain is used in atomization devices, including the spraying of large surfaces, for example, in insecticide application (Dombrowski & Fraser 1954), fire fighting and internal combustion engines (Mansour & Chigier 1990), where fuel burns as liquid drops (Lasheras & Hopfinger 2000). Injectors used in liquid rocket engines produce a liquid sheet (Magnus 1855; Dombrowski & Hooper 1964; Liu 2000) which disintegrates into

† Email address for correspondence: graeme.jameson@newcastle.edu.au

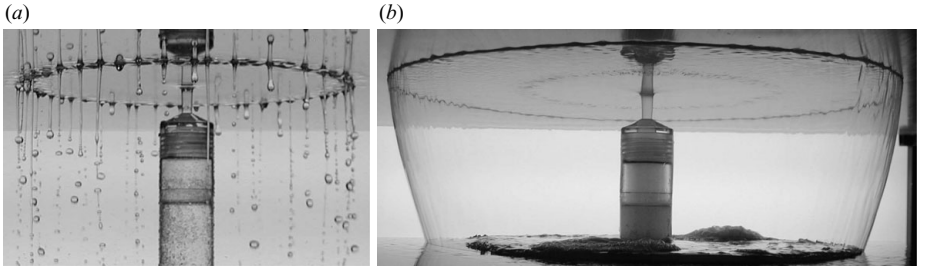

FIGURE 1. After the fluid departs the plate, it may fall in threads or coalesce to form a water bell. (*a*) Liquid thread configuration occurs with water; (*b*) a bell is created after the addition of surfactant. The nozzle cylinder is 60 mm in diameter, and the volumetric flow rate of the jet is (*a*) 7 L min^{-1}, (*b*) 19 L min^{-1}.

drops. This atomization was studied by Bremond & Villermaux (2006) and Bush & Hasha (2002).

Here, we report the discovery of a new type of water bell (Jameson *et al.* 2008). A liquid jet was directed vertically upwards at a large horizontal plate. From the point of impact, the fluid spread radially to an abrupt point on the flat surface of the plate, and then departed of its own accord. The fluid then fell in threads, or coalesced to form a water bell (see figure 1). These water bells, and the abrupt departure of the radial flow generated along the bottom of the horizontal plate represent new phenomena. The primary difference between these water bells formed on the underside of a horizontal plate, and those in all previous studies, is the point at which the free liquid curtain begins. In all previous studies, the point of departure of the bell has been specified by some physical aspect of the system; in most cases, the direction of departure has also been specified. Thus when a jet impinges on a flat horizontal disk, the bell departs from the edge of the disk whose radius is known. In the present case, the point of departure from the horizontal plate is determined purely by fluid dynamical conditions. These new water bells also display pronounced hysteretic effects. Once a bell has been formed, many interesting and beautiful shapes are produced if the flow rate of the impinging jet is altered. In this paper we report in detail observations of this new phenomenon, while theories are described in a companion paper (Part 2, Button *et al.* 2010).

Experimental study of water bells began in 1833, with the work of Savart, who considered several related problems: the breakup of liquid jets (Savart 1833*a*), the impact of a liquid jet on a disk and the resultant formation of water bells (Savart 1833*c*), the impact of a liquid jet on a plate and the formation of a hydraulic jump (Savart 1833*d*), and the liquid sheet created when two co-axial jets collide (Savart 1833*b*). In particular the formation of liquid sheets and hydraulic jumps formed by the impact of a liquid jet on a disk or plate are relevant to water bells formed on the underside of a horizontal plate.

A liquid jet falling on to a horizontal plate is commonly observed, perhaps most regularly in an empty sink. Upon impact, the fluid spreads radially in a thin layer before a circular hydraulic jump results in an abrupt depth increase. Rayleigh (1914) reported the existence of circular jumps, and investigations into their nature have been conducted by Watson (1964), Olsson & Turkdogan (1966) and Liu & Lienhard (1993). Interest has been revived more recently, with the discovery of non-circular jumps. Ellegaard *et al.* (1998), Aristoff *et al.* (2004) and Bush, Aristoff & Hosoi (2006) report on asymmetrical shapes such as polygons, cat's eyes and clovers. While many

studies have been devoted to investigating a vertically falling liquid jet and its impact, there is a notable absence of work on the opposite problem – the impact of an ascending jet.

Many experimental observations regarding water bells have been made. Savart (1833*c*) investigated the effect of the diameter and velocity of the impinging liquid jet. These experiments inspired the set-up that was used by Clanet (2000, 2001). It was found that smaller jet diameters gave a more symmetric water bell. Savart (1833*c*) also reported the existence of water bell shapes containing a cusp, and discussed the stability of the liquid sheet. In particular, the gradual change in shape followed by the breaking of the liquid sheet was detailed. Savart (1833*b*) also mentioned another method for creating water bells – the collision of two co-axial jets of differing diameters. Bond (1935) used the breakup of liquid sheets as a means to measure surface tension, using the theory developed by Boussinesq (1869). Buchwald & König (1936) extended this idea to use water bells for the same purpose. The method was short lived, however, because Wegener & Parlange (1964) revealed flaws in the theory. Parlange (1967) provided several methods of solving the equations of motion to obtain the shapes of bells transformed when a jet falls on a disk. His solutions agreed well with the experimental shapes measured by Göring (1959). Hopwood (1952) renewed wide interest in water bells with a new experimental set-up: expelling fluid through an annular slit at the top of a tube. The basic water bell structure was a dome shaped bubble, but by altering the flow rate gradually, a succession of stable shapes were produced; some of these contained cusps. Hopwood noticed that puncturing the liquid sheet resulted in a sudden change in the shape. This was the first observation of a pressure difference across the surface of a water bell. The work of Hopwood was continued by Lance & Perry (1953), who integrated the equations of motion to obtain solutions for the shape of the bell, including the effect of the pressure difference. They also reported a personal communication of Hopwood to the effect that the pressure difference could be up to 0.1 cm of water. The water bell produced by Taylor (1959*a*) using a horizontal liquid jet showed the effect of gravity on the shape of the liquid sheet. In these experiments, the surface generated was not quite symmetrical, implying a weak gravity dependence.

It is often the case that a water bell is unstable. Once a mass of air is trapped inside the water bell, changing the conditions can induce a pressure difference across the liquid sheet. This pressure difference may become too large for a stable water bell to exist. In this case the film breaks, releasing the pressure, and a new water bell is formed. The stability of liquid sheets moving through air has been studied by Squire (1953) and Huang (1970) for a range of Weber numbers, and further investigation into cylindrical liquid curtain stability has been conducted by Crapper, Dombrowski & Pyott (1975), Jeandel & Dumouchel (1999) and Pirat *et al.* (2006). Clanet (2001) reported on water bell instabilities due to bulges in the shape of the bell, and pressure perturbations, as well as extensive work on the formation of a bell. Further examples of such instabilities were presented in Aristoff *et al.* (2006). This very recent interest has included polygonal water bells (Buckingham & Bush 2001) and 'transonic' water bells (Brunet *et al.* 2004). The latter involved creating a water bell by overflowing a dish full of liquid. This method allowed bells to be created at much lower fluid velocities. These water bells exhibit the greatest similarities with those formed on the underside of a horizontal plate. When a transonic water bell was formed from the overflow of a dish, and then underwent a change in flow rate, the bottom of the bell surface was seen to creep up the central pipe. The volume of air inside the bell appeared to remain constant throughout this change. For these water

bells, however, the change in shape through such a process was much less pronounced than for those formed on the underside of a plate, reported here. This is due to the fact that the fluid curtain must always begin at the same location (the edge of the dish), leaving less room for change in the bell size and shape. Brunet *et al.* (2004) also reported on the transition from a water bell to a circular array of liquid threads at very low flow rates. This arrangement of columns has been studied in more detail by Giorgiutti & Limat (1997) and Brunet, Flesselles & Limat (2001, 2007). Similar water bells formed by allowing liquid to fall through an annular orifice were studied by Baird & Davidson (1962*a*,*b*). Other novel water bell types exist, including swirling water bells (Bark *et al.* 1979; Gasser & Marty 1994), reverse water bells (Engel 1966; Thoroddsen 2002) and several more described in Clanet (2007).

In this paper we present experiments in which water bells are formed on the underside of a horizontal impact plate. In § 2, the apparatus and procedures are described. General observations on the behaviour of the bells, particularly the response to changes in flow rate, are given in § 3. Both the radius of the impact circle of the impinging jet and the angle of departure from the horizontal plate are found to be functions of the flow rate, and strong hysteretic effects are noted. Quantitative results for the departure radius, angle, bell shape and range of stability are presented in § 4. Some data are given for cases where the bell was open and closed to the atmosphere, and the thickness of the liquid curtain is investigated. Conclusions are presented in § 5. Theories for some of the observed phenomena are presented in a companion paper (Part 2, Button *et al.* 2010).

2. Experimental method

The general set-up of our experimental apparatus is shown in figure 2(*a*). A water bell was formed when the liquid jet impinged on the underside of the impact plate. The impact plate itself was square, with side length 1 m, which is much larger than the region in which the water bell formed. Two different impact plates were used: one glass with a Teflon coating, the other simply clean glass. The plate was mounted horizontally and centred 40 mm above the jet nozzle. Jet nozzles of radius 3, 4 and 5.5 mm were used. A smooth tapered inner nozzle surface served to suppress turbulence. After forming the water bell, the fluid fell by gravity into the catchment, and was then directed back to the reservoir, a 90 L perspex container. Flow was then driven by a small electric pump (Model CP25, Mono Pumps Australia Pty. Ltd, Melbourne, VIC, Australia). A closed vertical column, of internal diameter 25 mm and height approximately 2 m, was used to dampen any mechanical noise created by the pump. Fluctuations in the height of the liquid in this column were less than 1 mm. The flow rate was measured with a magnetic flowmeter (Model Admag SE, Yokagawa Australia Pty. Ltd, Newcastle, NSW, Australia). The liquid was recirculated, so that its characteristics could be kept constant. Piping with an internal diameter of 25 mm connected all the previously mentioned pieces of apparatus. Three different fluids were used: two glycerol–water mixtures (70–30 and 90–10 w/w) and a surfactant (Triton X-100, 0.16 mM) solution. The properties of these liquids are summarized in table 1. The temperature of the liquids in the reservoir was monitored repeatedly throughout the experiments, and was recorded along with the fluid properties.

A Nikon D100 SLR digital camera, mounted on a tripod, was used to take images of the water bells. A diffuse light source located behind the water bell increased the contrast in these photographs. In some experiments, a tube was used to break the liquid sheet, and allow the pressure to equalize. Additional air was also added to

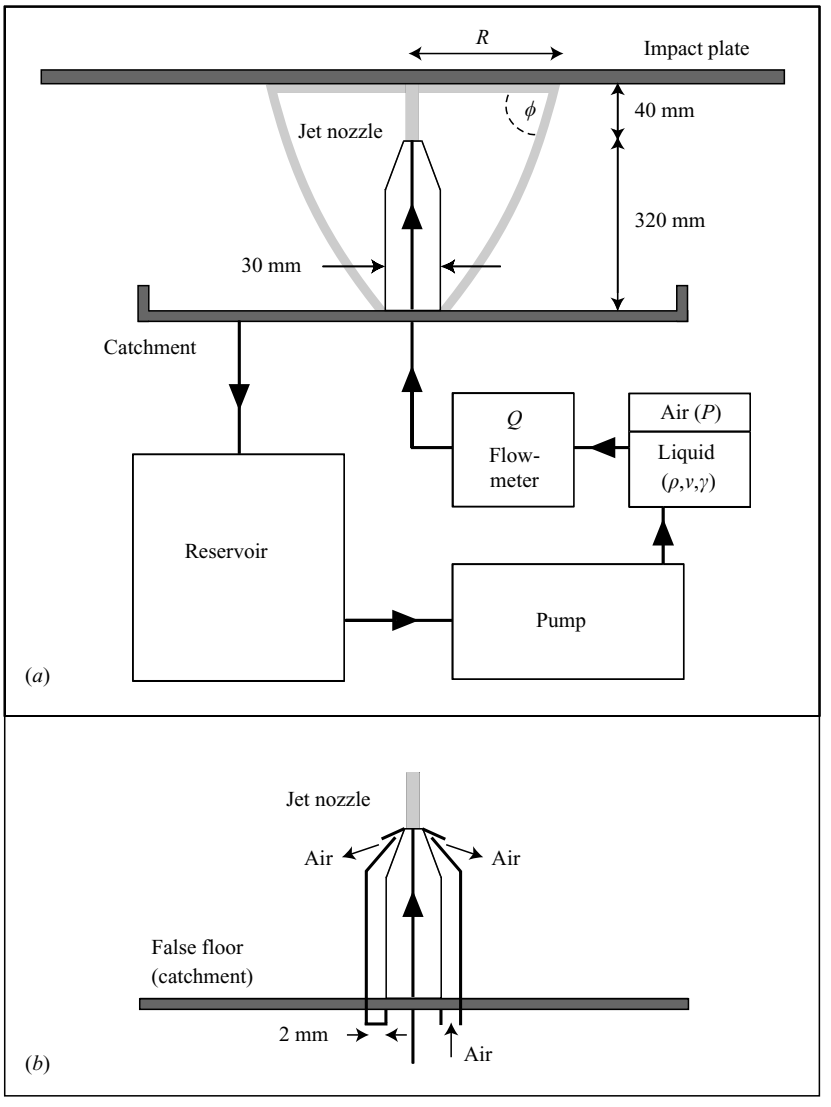

FIGURE 2. (*a*) A schematic illustration of the experimental set-up. (*b*) Removable nozzle attachment designed to inject air inside the bell.

the inside of the bell in this way. For use in one investigation, a nozzle attachment was designed to inject air into the bell without disrupting the liquid sheet. An apparatus was constructed in which a parallel-sided step was formed in the sloping face of the nozzle tip, adjacent to the exit orifice. A ring of small holes was drilled into the vertical face of the step, to allow air flow into the bell from an internal cavity. The air was directed radially outwards. This nozzle attachment is illustrated in figure 2(*b*).

In general, the procedure consisted of forming water bells at various flow rates. On some occasions it was difficult to form a coalescent sheet, and rapidly increasing and decreasing the flow rate achieved stability. Several photographs were then taken of the bell, an average of which would later provide the quantitative measurements. Five photographs were used for most measurements, to eliminate the effect of fluctuation in lighting. Photographs were analysed computationally using the software

	ρ (g cm^{-13})	ν (cS)	γ (N m^{-1})	T (°C)
70–30 (w/w) glycerol–water	1.16	20.7	0.067	19
90–10 (w/w) glycerol–water	1.24	99.3	0.065	28
Triton X-100 solution	1.00	1.1	0.033	22

TABLE 1. Fluid properties. Density ρ, kinematic viscosity ν, surface tension γ and the temperature at which the experiments took place T.

package Adobe Fireworks (Adobe Systems Inc., San Jose, CA, USA). This allowed measurements such as departure radius and water bell volume to be determined accurately. Since the diameter of the central nozzle was known, this was used as a reference scale in all photographs. In some cases the water bells became unstable after only a short period of time; the origin of this intermittent stability is unknown. This meant observing hysteretic effects over a large range of flow rates was not always possible. In some cases, video was used rather than photograph in order to capture these dynamic effects. Data measurements were taken from these videos in the same way as from the photographs.

Triton X-100 solutions (0.16 mM was used – the critical micelle concentration is 0.24 mM) were used for some of the experiments. Such a solution was used to form water bells of a low viscosity, as this was not possible with pure water. Concerns about the effects of surfactants on dynamic surface tension, as well as potential uncontrollable Marangoni stresses meant that glycerol–water mixtures were used for the majority of our study. The Triton X-100 results are discussed nonetheless.

3. General observations

Extensive observations of the water bells were made under numerous conditions, in order to elucidate the mechanisms driving the flow. Of particular interest were (i) the flowing thin film that spread radially outwards from the impingement point along the plate, (ii) the angle of departure from the plate and (iii) the existence, stability and shape of the liquid sheet. These observations are detailed below.

3.1. *The radial thin film flow*

Water bells were formed at a variety of flow rates, Q. The outer radius of the circular thin film was seen to be strongly dependent on Q. For low flow rates, the thin film flow along the plate did not extend sufficiently far from the impinging jet for a bell to form. In addition to this, it was only possible to form a stable water bell for flow rates beneath some critical value, presumably due to turbulence. Both the minimum value and where the instability first occurred were dependent on the fluid, and so the range of flow rates considered in the experiments varied accordingly. A 70 % glycerol mixture was able to sustain stable bells for $Q \in (2, 20)$ L min^{-1}, a 90 % glycerol mixture for $Q \in (8, 21)$ L min^{-1} and a Triton X-100 solution for $Q \in (3, 20)$ L min^{-1}. The relationship between flow rate and departure radius was investigated experimentally for Q in the range appropriate for a given fluid. For every water bell seen experimentally, an increased flow rate resulted in a larger departure radius. This was true for the flow on the underside of the plate whether the fluid formed a stable bell, an unstable bell or fell in threads. Given the substantial overlap in the stable range of flow rates for the different liquids, a comparison between the relevant departure radii can be made. Viscosity could be most easily changed, and in this

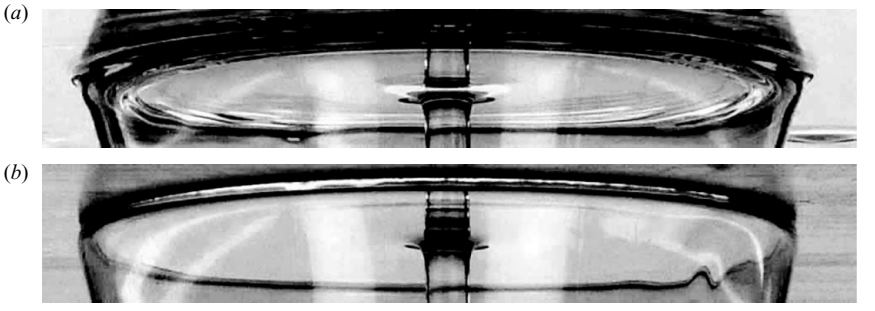

FIGURE 3. Thin film along the underside of the plate. Flows generated using 70 % glycerol mixture pumped through a jet of 4 mm radius at $Q = 6.7$ L min^{-1}; (*a*) glass surface, (*b*) Teflon surface.

investigation there was a range of two orders of magnitude in the fluids considered. A consistent relationship was observed at all applicable flow rates – the greater the viscosity of the fluid, the smaller the departure radius. Increasing the viscosity by a factor of 100 caused the departure radius to change by approximately a factor of 4. Altering the concentration of Triton X-100 in the surfactant solution acted to change the surface tension, while having negligible effect on density and viscosity. Increasing the concentration by 30 %, and hence reducing the surface tension of the liquid–air interface by approximately 10 %, resulted in an increase in the departure radius of roughly 3 %. The consequence of varying the radius of the impinging jet was investigated, and this appeared to have no effect. The maximum radial extension of this thin film therefore appeared to depend strongly on the flow rate of the impinging jet, have a weak inverse relationship with both viscosity and surface tension and be independent of the jet radius.

Finally, the nature of the solid surface itself was considered. Water bells were created with a 70 % glycerol mixture on both glass and Teflon coated surfaces. There was no noticeable difference in the dimensions of the bell. At the departure radius, the liquid made a local contact angle, θ, with the solid that was dependent on the nature of the surface. Figure 3 highlights the difference in local contact angle formed on hydrophilic (glass) and hydrophobic (Teflon) surfaces. This angle was determined by drawing tangents to the interface at the contact point on a photograph with a magnification of 5×. An example of this method is presented in figure 4. For a 70 % glycerol mixture, the contact angle was measured to be approximately 34° on glass and 116° on Teflon. The local contact angle was measured for flow rates across the entire range at which a stable bell could be formed. As shown in figure 4(*c*), there was no change in angle over this range. All these measurements were taken when the bell was in a static position, that is, the flow rate was held constant. The local contact angle appeared to decrease slightly at times when the flow rate was being decreased, and increase slightly when the flow rate was being increased. Since the position of the contact point changed with flow rate, this observation was consistent with the well-known feature of advancing contact angles being larger than receding contact angles.

The measured local contact angle should be considered with reference to the equilibrium contact angle of a droplet of 70 % glycerol mixture sitting on the surface. The equilibrium contact angle was measured to be 80.0(±0.3)° on Teflon and 19.0(±1.5)° on glass. These angles were determined using a Data Physics Contact Angle System, Model 0CA20, Data Physics Corporation, San Jose, CA, USA. Thus the

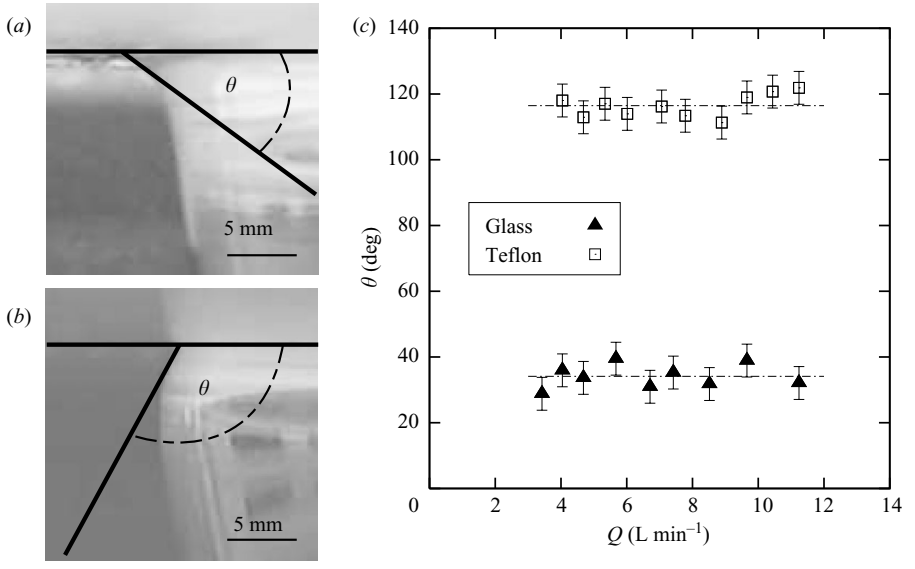

FIGURE 4. Contact angle formed at the rim of the radial flow. Determination of the angle is shown on (*a*) glass, (*b*) Teflon, (*c*) results for a range of flow rates.

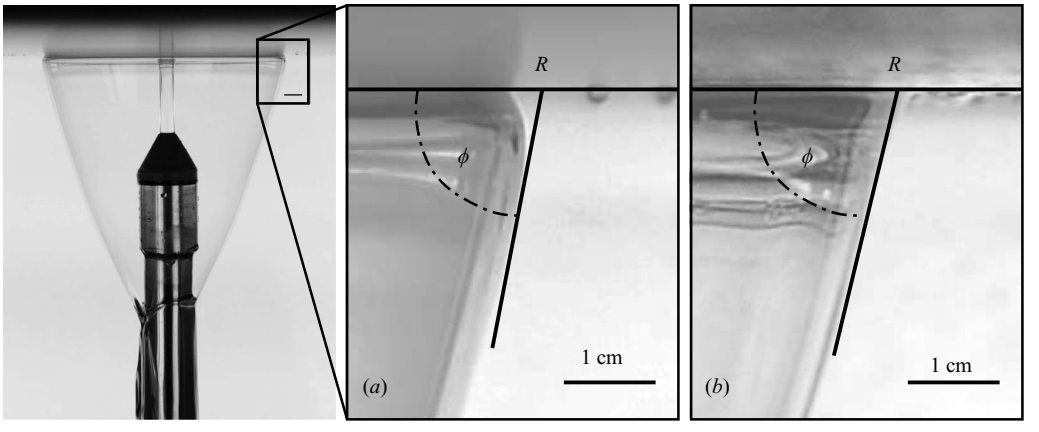

FIGURE 5. Illustration of the measurement of departure radius R and departure angle ϕ on (*a*) Teflon, (*b*) glass.

local contact angle observed in the water bells depends on the nature of the surface, being larger than the value measured for a static droplet. These measurements are consistent with enhanced local contact angle in comparison to equilibrium due to finite momentum flux through the film.

Critically, this microscopic difference does not cause any noticeable change in the macroscopic appearance of the water bell. The radial dimension of the bell is independent of the nature of the surface, as is the shape of the liquid curtain, and the departure angle ϕ (see figures 2 and 5).

In some cases, standing waves were visible in the thin film flow. These can be seen as rings near the departure radius in figure 3(*a*). These waves were observed only in the bells produced on a glass surface. A close-up of the film generated on a Teflon surface is shown in figure 3(*b*), where standing waves are not visible to the naked eye.

3.2. *Departure from the plate*

When the fluid departed the plate, it either fell in threads or coalesced to form a water bell (see figure 1). It was not always physically possible to form water bells; coalescence depended on the liquid properties. Importantly, it was not possible to form water bells using pure water. It is noted that both increasing viscosity and reducing surface tension could induce coalescence. A thorough investigation into the transition from liquids that form threads into liquids that form a curtain was not undertaken, since this study is concerned with the behaviour of the formed water bells. The stability of formed water bells is investigated in § 4.2.1.

At the point of departure from the plate, a sharp angle ϕ was formed between the solid surface and the falling film (see figure 5). This water bell departure angle is not the local contact angle θ, described above, and applies a finite distance below the solid surface. The departure radius R and angle ϕ were measured by drawing a tangent to the water bell 1 cm below the solid surface, as shown in figure 5. This avoided the interference of the local contact angle θ in the determination of the macroscopic dimensions of the water bell. The curvature of the bell surface in this region is low, and hence the choice of 1 cm below the solid surface as the location for the tangent provides an accurate description of the water bell departure angle. It should be noted that the recorded departure radius R will differ from the exact radius at which the liquid leaves the solid surface by up to 5 mm due to this definition (see figure 5). This definition has been chosen in order to capture the large-scale behaviour of the water bells.

When a water bell was initially formed, and so the inner and outer pressures were equal, the water bell departure angle ϕ was typically in the range $60^\circ < \phi < 90^\circ$. This angle was not strongly dependent on the flow rate of the impinging jet. The departure angle did not appear to be strongly dependent on either the departure radius or the nature of the surface; this is investigated in § 4.1.1.

In contrast, for the case of closed bells – those with internal air cut off from the atmosphere – ϕ was heavily dependent on the ratio between the current volumetric flow rate Q and the volumetric flow rate at which the water bell was initially formed, Q_0. Increasing the flow rate corresponds to $Q/Q_0 > 1$, whereas decreasing the flow rate yields $Q/Q_0 < 1$. The most interesting observations regarding the departure angle occurred when the flow rate was altered. When the flow rate was increased ($Q/Q_0 > 1$), the departure angle ϕ decreased, and became very small. In the opposite case of decreasing flow rate, $Q/Q_0 < 1$, ϕ could increase to values above 90°. Water bell departure angles were observed in the range $30^\circ < \phi < 100^\circ$. By comparing the departure angles of open and closed water bells, significant insight into the mechanism at play can be deduced, as will be discussed.

Azimuthal striations were observed in the liquid curtain in some cases. These can be seen in figure 1(*b*). It is not known what caused these striations, and a thorough investigation into their nature is yet to be performed.

3.3. *Water bell shape*

Once a water bell had formed, and the flow rate was altered, many interesting shapes were produced. Two series of water bell shapes are presented for comparison. These serve to illustrate effects of the entrapped air inside the bell.

Figure 6(*a*) shows a series of stable closed water bells. The initial bell was formed using a 70 % glycerol mixture at a flow rate of 5.9 L min^{-1}. The falling fluid coalesced into a sheet, trapping a fixed amount of air inside the bell. The flow rate was then

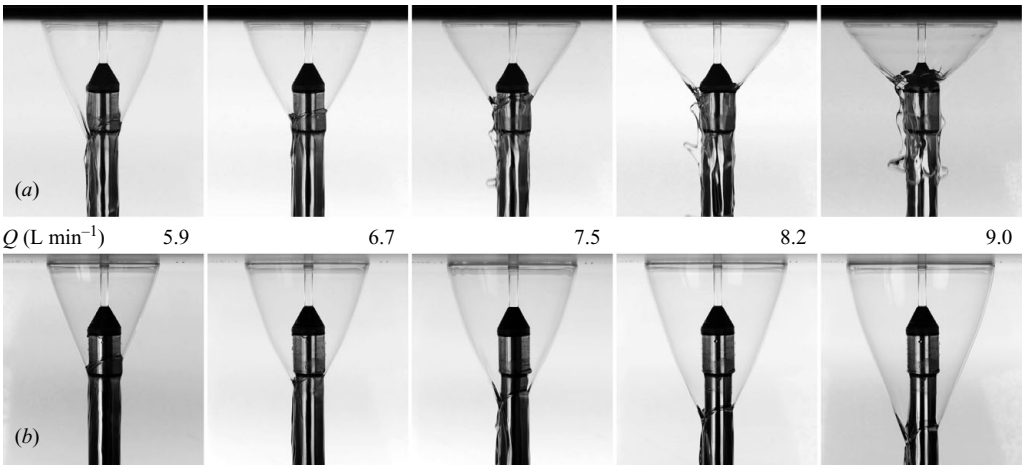

FIGURE 6. Change in water bell shape with increasing flow rate. (*a*) Air is trapped inside the bell throughout the increase in flow rate. (*b*) Surface is broken with a tube between photographs. Time interval between frames is 5 s. Bells formed using 70 % glycerol mixture, 4 mm jet radius and Teflon surface.

steadily increased to 9.0 L min^{-1}. While the radius of departure increased, as expected, the water bell itself changed shape markedly.

The internal volume was forced to remain constant throughout this series of water bells. As the radius of the departure point on the top plate increased, the bottom of the bell crept up the central pipe. A similar phenomenon was observed in the opposite situation. When a water bell was formed and the flow rate steadily decreased, the departure radius also decreased. The base of the bell then crept down the central pipe, also conserving volume. While a particular water bell remained stable, the volume inside was constant and this hysteretic effect was observed. The resulting shape was dependent upon both the current flow rate and the conditions of original bell formation.

Another interesting observation was made when the surface of such a bell was pierced. Any break in the sheet acted to immediately end the hysteretic behaviour. The water bell then reverted to the shape it would take had it been originally formed at that flow rate. This suggested a pressure difference was induced across the surface of the bell, and that the pressure difference was responsible for the hysteretic effects. Breaking the surface would allow the internal pressure to equilibrate with the atmosphere and the bell to take its natural shape.

The series of water bells shown in figure 6(*b*) was produced by piercing the surface of the bells with a tube between successive photographs. This ensured the internal and external pressures were identical in each of the photographs. The behaviour of these bells was very different, no hysteresis or volume conservation was observed.

For any given flow rate, a wide range of bell shapes were possible – this depended on the flow rate at which the air inside the bell first became trapped. Figure 7 shows three water bells existing at the same flow rate, but displaying different sizes and shapes due to different initial flow rates. For example, the water bell shown in figure 7(*a*) was initially formed at a flow rate of 17.3 L min^{-1}, and then the flow rate was decreased to 6.7 L min^{-1}. The air remained trapped inside the bell throughout the transformation.

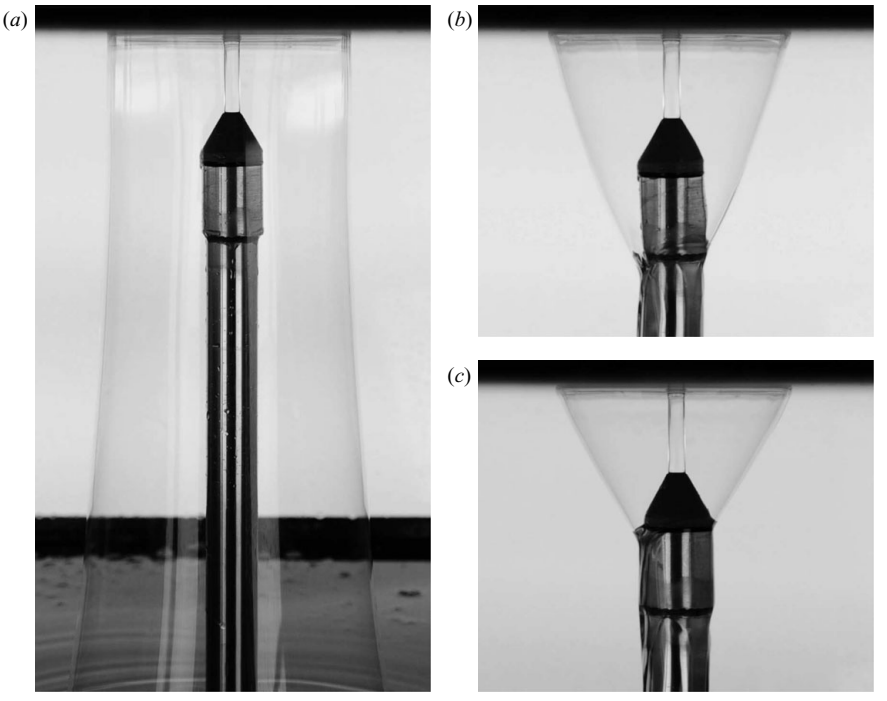

FIGURE 7. Hysteresis in water bell shape: all bells formed at a flow rate $Q = 6.7$ L min^{-1}, with a 70 % glycerol mixture, 4 mm jet radius and Teflon surface. The initial flow rate Q_0 was (*a*) 17.3 L min^{-1}, (*b*) 6.7 L min^{-1}, (*c*) 5.3 L min^{-1}.

3.4. *Existence of the liquid curtain*

The liquid sheet became unstable in several cases, broke, and a new water bell formed. If the flow rate was increased sufficiently, having initially taken a small value, the bottom of the sheet passed the top of the pipe and contacted the jet. The base of the water bell rose, and eventually there was no solid surface to support it. At this time a new, larger water bell formed, whose lower contact circle was well below the issue point of the jet.

Another type of instability was coerced by reducing the flow rate. This reduced the departure radius and the lower part of the bell surface crept down the pipe, conserving the initial volume. If the flow rate was decreased sufficiently, the bell surface contacted the catchment plate in some cases. The lower part of the bell surface then expanded radially. An example of this situation is shown in figure 7(*a*). It was in this case that departure angles $\phi > 90^\circ$ were observed. As the flow rate was decreased further, the base of the liquid sheet eventually expanded so far that it became unstable. The sheet dilated at the bottom, and eventually jumped off the bottom surface. This allowed air to escape underneath and thus eliminated any pressure difference between the interior and exterior of the bell. A new water bell of smaller size then formed. The liquid sheet remained whole everywhere except at the location of the jump instability in the sheet. A continual reduction in flow rate caused this behaviour to be repeated, the size of the water bell reducing each time.

3.5. *Relationship between departure radius and angle*

To examine the mechanism causing the radially expanding thin film to depart the top plate, we studied (i) the relationship between the departure radius and departure

angle and (ii) the path taken by the fluid subsequent to its departure. We considered the case of a stable water bell formed at a constant flow rate of 10 L min^{-1}. Using the special attachment to the nozzle, described in § 2, air was pumped into the bell at 3 L min^{-1}. Consequently, the shape of the water bell surface changed dramatically. As the volume of the bell increased, the departure angle underwent substantial change. Photographs of this phenomenon (extracted from video), taken at uniform time intervals, are shown in figure 8. Noticeably, the critical radius where the fluid left the plate, remained constant throughout this process. This is an important observation, because it illustrates the independence of departure radius and angle under such conditions. This suggests that the flow rate determines the specific point at which the flow along the bottom of the plate must depart the surface, and the direction in which it falls is of little importance. This was also consistent with observations made when air was simply blown into a bell using a tube.

4. Quantitative results

The above observations indicate a clear distinction between water bells at the initial flow rate ($Q = Q_0$), and bells at other flow rates where air is trapped ($Q \neq Q_0$). The first situation occurred when (*a*) the pump was turned on at a particular flow rate, and a water bell formed or (*b*) occurred when the surface of the water bell was broken by a tube, and any internal–external pressure difference was eliminated. The second situation occurred when the flow rate was changed after a volume of air had been trapped; in this latter case hysteretic effects were observed (see § 3.3). Quantitative results are presented first for bells with $Q = Q_0$, in order to gain an understanding of the fundamental flow phenomenon, following which hysteresis is examined.

4.1. *Water bells without hysteresis* ($Q = Q_0$)

4.1.1. *Departure radius*

Here we investigate the quantitative value of the water bell departure radius as a function of the impinging jet flow rate. The procedure for obtaining these measurements was as follows. A water bell was formed at a particular flow rate, and the liquid sheet was broken with a tube. The curtain was allowed to close again, trapping a mass of air. This ensured that $Q = Q_0$, and there was no pressure difference across the surface of the bell. Photographs were taken of the water bell at this time. The flow rate was then increased slightly, the liquid sheet was broken again with a tube and further photographs were taken at the new flow rate. This process was repeated until stable water bells could no longer be formed (see § 3.1). The flow rate was then decreased systematically to the minimum possible flow rate, with images being taken at regular intervals. The entire protocol was repeated several times. The departure radius, as defined in figure 5, was determined using the photographs and the software package Fireworks. The known diameter of the central pipe was used as an accurate scale for the photographs. At a given flow rate, the average of all measurements was taken for the departure radius. This protocol was implemented using each of the three fluids described in § 2. The results can be seen in figure 9(*a*). Results for a 70 % glycerol mixture were obtained using both glass and Teflon surfaces; this data is also shown in figure 9(*a*). The nature of the surface (glass or Teflon) appeared to have no effect on the departure radius.

To investigate the effect of the velocity of the impinging jet, water bells were formed using three different nozzle radii. A 70 % glycerol mixture was used to form water bells over the range of flow rates using 3, 4 and 5.5 mm nozzle radii. The

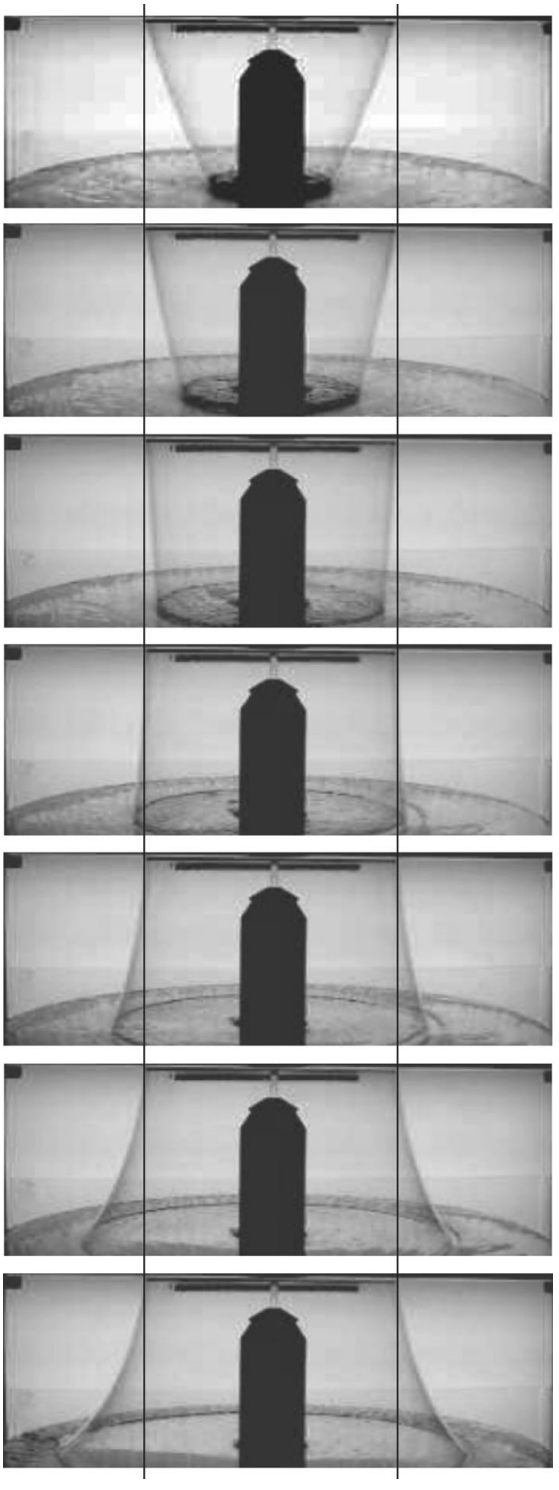

FIGURE 8. Analysis of water bell departure radius and angle. Liquid curtain formed at $Q =$ 10 L min^{-1}, using Triton X-100 solution, 4 mm jet radius and Teflon surface. Air was added to the inside of the bell. Time interval between frames is 30 s.

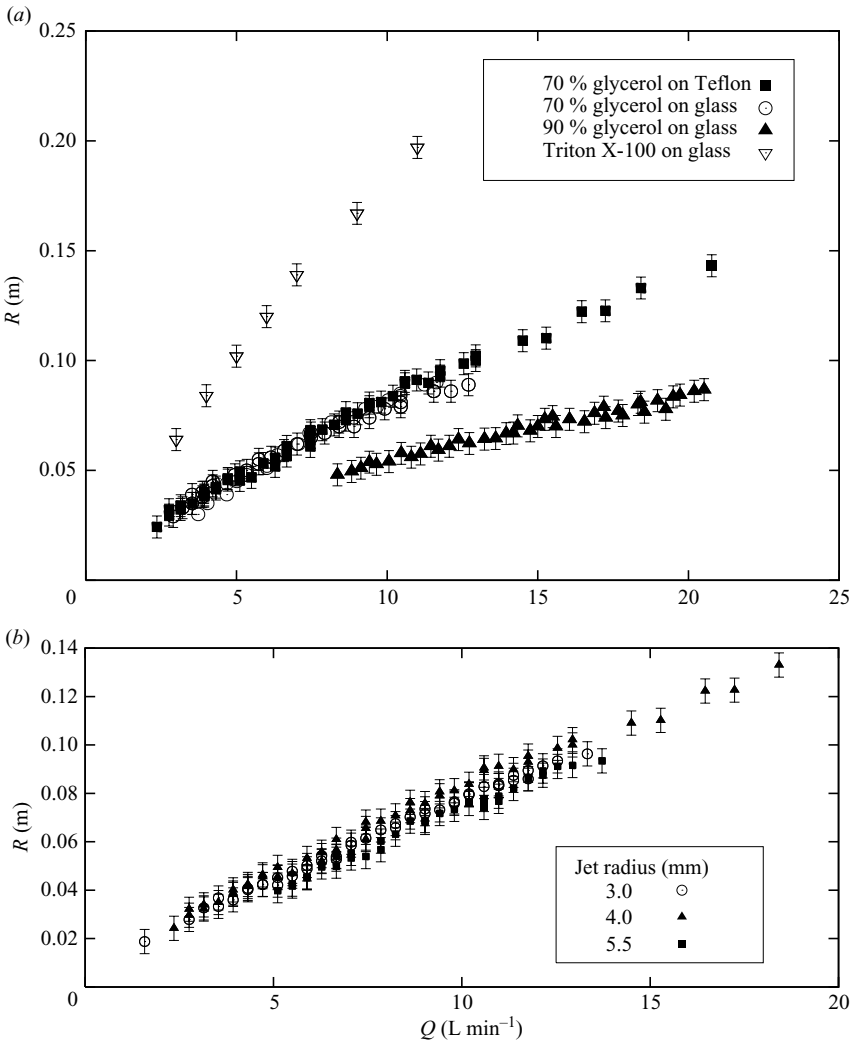

FIGURE 9. Departure radius at different flow rates for three fluids. (*a*) Results using 4 mm jet radius, (*b*) results using 70 % glycerol mixture on Teflon.

departure radius was found to be identical to within experimental error in all cases. We therefore conclude that the departure radius depends on the volumetric flow rate of the impinging jet, but not on the fluid velocity or jet diameter.

A dimensional analysis was conducted on the experimental results for departure radius to probe the functional dependence on the various parameters. The following assumes that the departure radius R depends only on the density ρ, kinematic viscosity ν, surface tension γ and volumetric flow rate Q of the liquid. The system can be described using two dimensionless groups of the form $\pi_i = \rho^{m_1}\nu^{m_2}\gamma^{m_3}Q^{m_4}R^{m_5}$, where the m_j are to be determined (Bridgman 1931). The resulting dimensionless groups are $\pi_1 = Q\gamma(\rho\,\nu^3)$, $\pi_2 = R\gamma/(\rho\,\nu^2)$. The Buckingham π theorem states $f(\pi_1, \pi_2) = 0$ for some function f, or alternatively, $\pi_2 = \Upsilon(\pi_1)$ for some function Υ. π_2 is plotted as a function of π_1 using experimental data to investigate the functional form of Υ. Figure 10 shows data used in figure 9(*a*), and in this form all the points

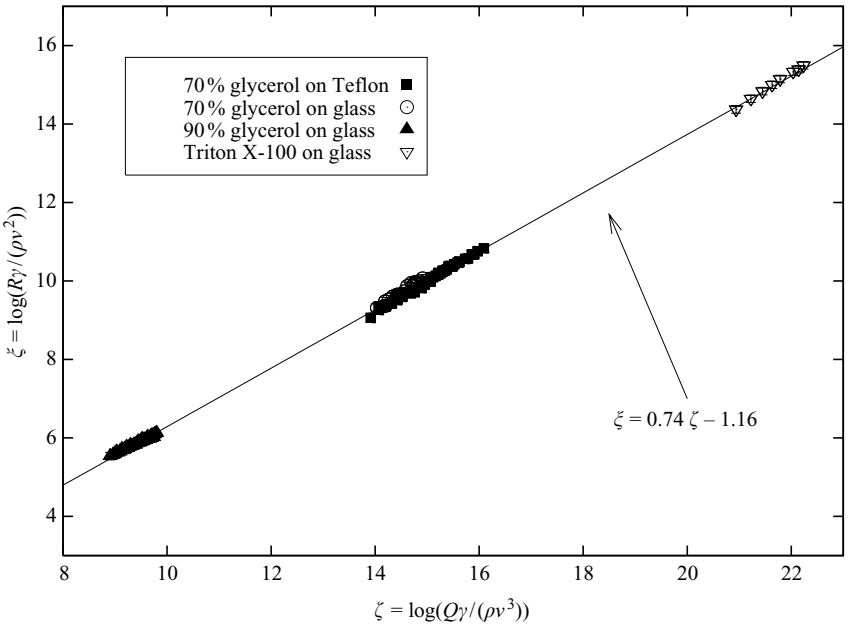

FIGURE 10. Dimensional analysis of departure radius. Standard deviation from the fit is 0.021.

collapse on to a straight line. A linear fit to this log–log data gives $\pi_2 = \mathrm{e}^{-1.16}\pi_1^{0.74}$ or $R\gamma/(\rho v^2) = 0.31\,(Q\gamma/(\rho v^3))^{0.74}$, i.e.

$$R = 0.31\left(\frac{\rho^{0.26}Q^{0.74}}{\gamma^{0.26}\nu^{0.23}}\right). \tag{4.1}$$

We emphasize that this is an empirical fit, the origin of which will be investigated in Part 2 (Button *et al.* 2010).

4.1.2. *Departure angle*

The departure angle was measured over the range of flow rates for which a stable bell could be formed. Using a 70 % glycerol mixture, water bells were formed at a particular flow rate, and the surface broken to ensure no pressure difference existed across the surface. Photographs were taken of the bell before the flow rate was adjusted to a new level, and the procedure repeated. Angles were then determined from the photographs, using tangents drawn 1 cm below the surface, as shown in figure 5. Each data point represents the average of the left and right departure angles for each of the photographs. This method was implemented using both glass and Teflon surfaces. The results are presented in figure 11, where it is seen that the nature of the surface has no observable effect on the departure angle. It is also noted that the departure angle is weakly dependent on the flow rate of the impinging jet. The angle increased by approximately 20 % as the flow rate was increased from its lowest value to its highest.

4.1.3. *Bell shape*

The shape of the liquid curtain was extracted from photographs in the following way. Intensity of the photograph was first inverted using Fireworks, and then the levels adjusted to improve contrast (see figure 12). A grid was then placed over the

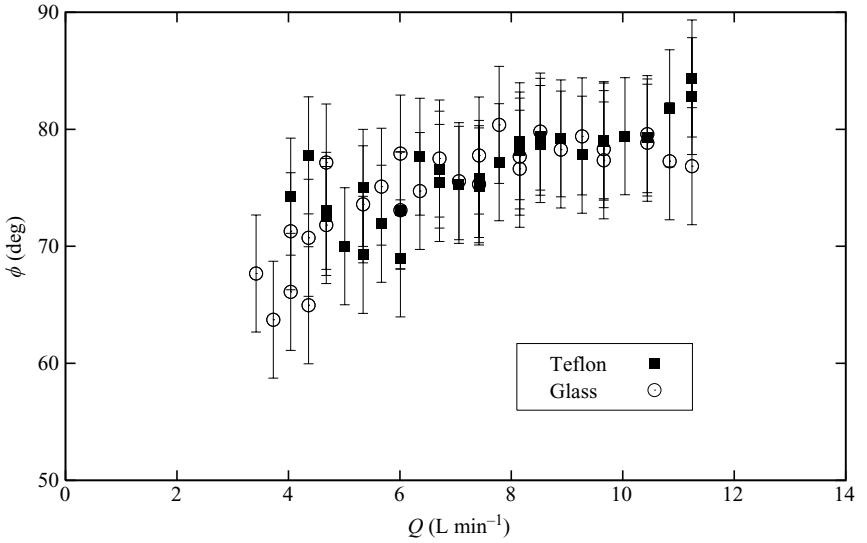

FIGURE 11. Departure angle. Data obtained using 70 % glycerol mixture pumped through a jet of radius 4 mm.

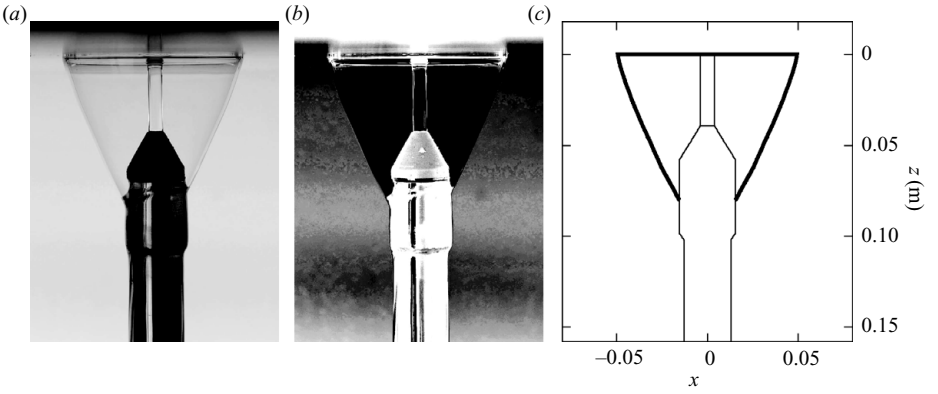

FIGURE 12. Method of extraction of water bell shape. (*a*) Original photograph, (*b*) inverted and adjusted contrast levels, (*c*) extracted shape.

top of the photograph, allowing the position of the surface to be measured at equally spaced points. The grid had spacing equivalent to 0.2 mm, allowing the shape to be accurately determined to this level. The diameter of the central pipe was again used as a reference scale. Figure 13 shows the bell shape obtained using 4 different flow rates. The shapes are qualitatively similar, but they increase in size with the flow rate.

4.2. *Water bells with hysteresis* ($Q \neq Q_0$)

The hysteretic behaviour of these water bells are now investigated. In the following experiments, the liquid curtain was not broken between subsequent data measurements, allowing a pressure difference to be induced across the surface. The physical origin of some of these observations is studied theoretically in the companion article (Part 2).

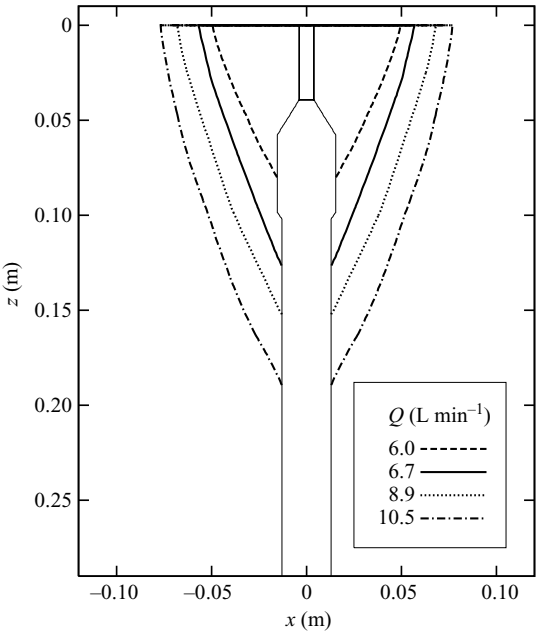

FIGURE 13. Bell shapes for a 70 % glycerol mixture, 4 mm jet radius and Teflon surface.

4.2.1. *Range of stability*

The first investigation was into the range of flow rates at which a stable hysteretic bell could be formed; the stability of non-hysteretic bells was discussed in § 3.1. A water bell was formed at a particular flow rate, and any pressure difference eliminated by puncturing the surface. This determined the value of Q_0. The flow rate was then slowly increased until the liquid curtain broke, to obtain the maximum flow rate Q_{max}, which could be sustained given the initial flow rate Q_0. A new water bell was then formed using the same value of Q_0, and the flow rate slowly decreased until it became unstable; this gave the minimum flow rate for which a bell could be sustained, Q_{min}. The phase space of stability is shown in figure 14, where each point represents the average of 5 experiments such as the one described above; the line $Q = Q_0$ is shown for reference. A vertical line at a particular initial flow rate Q_0 indicates how far the flow rate was altered from this value before the surface broke.

There are 4 different types of instability, or mechanisms for which a bell could no longer be formed. The numbers (1)–(4) in figure 14 indicate which of these instabilities occurred at that point; these are discussed below.

Region (1): The flow rate had been decreased sufficiently that the jet no longer reached the upper horizontal plate (impact plate in figure 2).

Region (2): The flow rate was less than the initial flow rate ($Q < Q_0$). As the flow rate was decreased, the bottom of the water bell surface crept down the central pipe, as illustrated in figure 7. The instability observed in this region occurred when the flow rate was decreased to a level that the bottom radius of the liquid curtain exceeded its top radius. The curtain became unstable at the point of contact with the bottom surface, and broke.

Region (3): The flow rate was greater than the initial flow rate ($Q > Q_0$). As the flow rate was increased, the base of the water bell crept up the central pipe. This

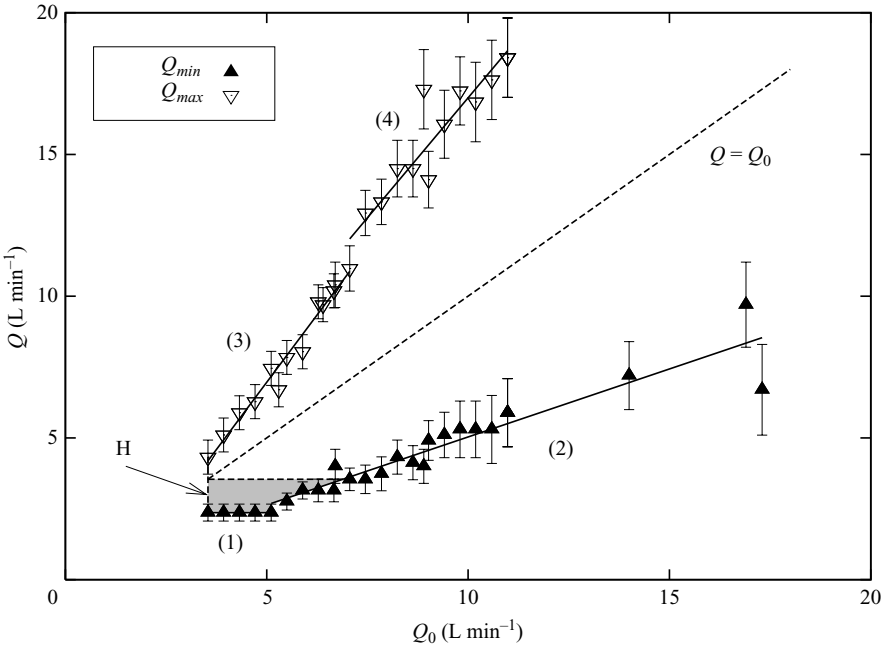

FIGURE 14. Range of flow rates a stable bell was formed given an initial flow rate. Data obtained using a 70 % glycerol mixture, 4 mm jet radius and Teflon surface. The region marked 'H' indicates that stable bells could be formed due to hysteresis only.

region shows those water bells that broke because there was no solid surface to support the base of the curtain, after it crept above the issue point of the jet.

Region (4): The base of the water bell had crept up the pipe and eventually became unstable of its own accord. As the base of the curtain crept up the pipe, azimuthal striations were observed in the film. Further increase appeared to induce turbulence in the liquid sheet, and eventually it broke.

It should be noted that regions (1) and (3) are largely a product of the particular geometry of our set-up. Regions (2) and (4) indicate that a genuine fluid dynamical instability occurred. The region marked 'H' shows flow rates at which a stable bell could be formed due to hysteresis only. These low flow rates could not sustain a water bell in the $Q = Q_0$ case, since the radial film did not extend significantly past the impingement point, and the falling film contacted the jet rather than the solid pipe. However, when a water bell was formed at a larger flow rate and hence a larger departure radius, and then the flow rate decreased, the liquid curtain extended further down and was able to contact the pipe. Using this method it was possible to create stable water bells at all flow rates down to the point at which the jet no longer reached the impact plate.

4.2.2. *Departure radius and angle*

An investigation was performed into the influence of hysteresis on the departure radius. Figure 7 shows photographs of three water bells, all at a flow rate of $Q =$ 6.7 L min^{-1}, but having been formed at different initial flow rates Q_0. If the departure radius was dependent only on the current flow rate Q, and not its history of formation, the departure radius would be identical in the case of these three bells. Figure 15(*a*) shows equivalent extracted shapes. It is clear that the departure radius was not the

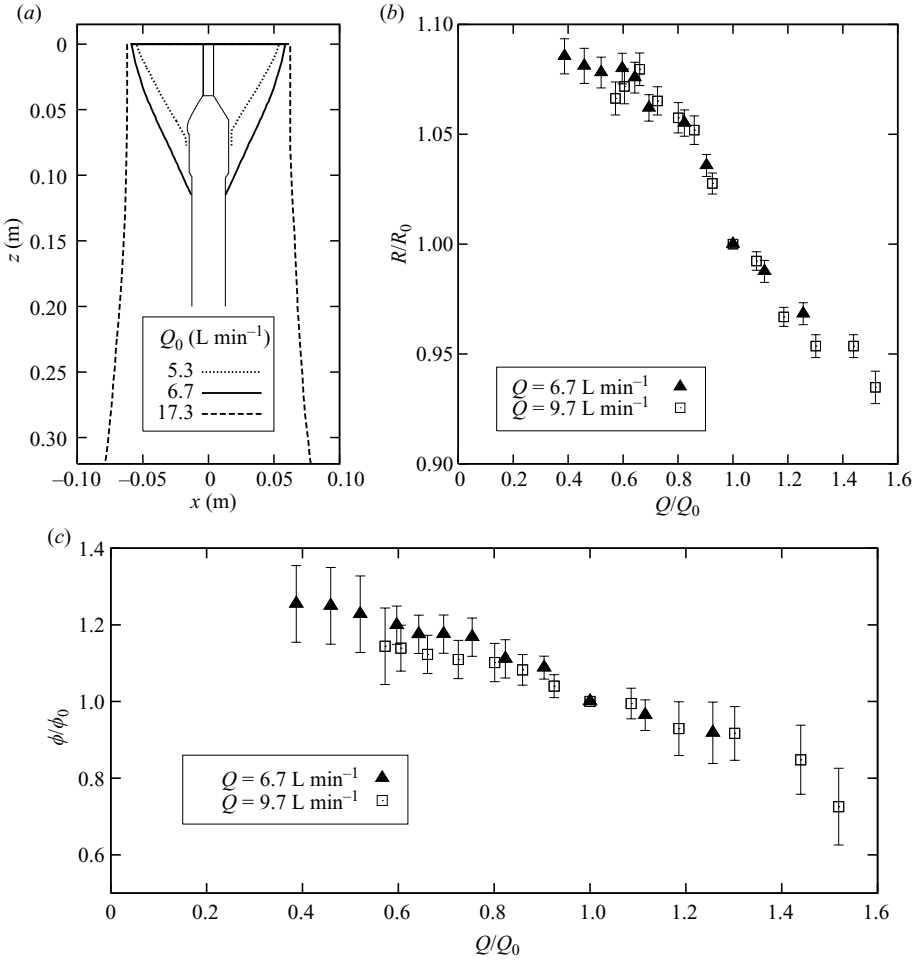

FIGURE 15. Effect of hysteresis on departure radius. (*a*) Extracted shapes at $Q = 6.7$ L min^{-1}, for various Q_0. (*b*) Relative change in departure radius due to hysteresis. R_0 is the departure radius obtained using $Q = Q_0$. (*c*) Relative change in departure angle. ϕ_0 is the departure radius obtained for $Q = Q_0$. Data using 70 % glycerol mixture, 4 mm jet radius and Teflon surface.

same in all cases, although considering the vastly different initial flow rates Q_0, the deviations are small. The value of the departure radius is considered with reference to the radius obtained for a bell with $Q = Q_0$. The radius was slightly larger in the case where $Q_0 = 17.3$ L min^{-1}, and slightly smaller in the case of $Q_0 = 5.3$ L min^{-1}. In general it was seen that for $Q < Q_0$, when the flow rate had been decreased, the radius was slightly larger. In the opposite case, $Q > Q_0$, the radius was slightly smaller than that obtained for $Q = Q_0$.

To obtain a quantitative understanding of the dependence of the departure radius on hysteresis, the following was undertaken. A water bell was formed at $Q =$ 6.7 L min^{-1}, and the surface punctured to ensure that there was no pressure difference across the surface of the bell ($Q = Q_0$). Photographs were taken of this water bell, and these were analysed to provide the reference data. An average of these photographs gave the departure radius, which shall be denoted R_0, to indicate the fact that it

is a measurement obtained using $Q = Q_0$. Another water bell was then formed at $Q_0 = 17.3$ L min^{-1}, and the surface punctured to eliminate any pressure difference. The flow rate was then slowly decreased until it was equal to 6.7 L min^{-1}. The air remained trapped inside the bell throughout this process. Photographs were taken at this time, and these were analysed to determine the resulting departure radius R. In both cases, $Q = 6.7$ L min^{-1}, but the value of Q_0 differed. This procedure was repeated to cover all initial flow rates Q_0, from which it was possible to adjust the final flow rate to 6.7 L min^{-1} without an instability occurring. Figure 15(b) shows R/R_0 as a function of Q/Q_0. It is noted that while the departure radius is influenced by the history of the water bell, the dependence is weak. Over the full range of flow rates, which corresponded to approximately a 60 % change, the departure radius changed by less than 10 % from the $Q = Q_0$ value. This experiment was repeated using the reference flow rate 9.7 L min^{-1}, and the data appeared to lie on the same curve. These results indicate that the hysteresis plays a relatively minor role in determining the departure radius.

In contrast, the extracted shapes in figure 15 show that the water bell departure angle is strongly dependent on hysteresis. The angle between the liquid curtain and the solid surface is much larger for the water bell created at 17.3 L min^{-1} than in the bell with an initial flow rate of 5.3 L min^{-1}. Using the photographs from the experiment described above, the effect of hysteresis on the departure angle was also investigated. Tangents to the bell surface were drawn 1 cm below the surface, and the departure angle determined. This data is presented in figure 15(c). We denote by ϕ_0 the value of the water bell departure angle for the case $Q = Q_0$, and the other angles are considered with reference to this. Decreasing the flow rate results in a significant increase in the departure angle, and increasing the flow rate results in a significant decrease in the departure angle. This was true for both reference flow rates, 6.7 and 9.7 L min^{-1}.

4.2.3. *Bell shape and volume*

To illustrate the effects of hysteresis on the water bell shape, two sets of measurements were produced.

(i) A closed water bell was formed using a 70 % glycerol mixture at flow rate of 6.7 L min^{-1}. The surface was punctured to ensure that there was no existing pressure difference. The flow rate was then steadily decreased to 4.7 L min^{-1}. As the flow rate decreased, the departure radius decreased, and the liquid sheet crept down the central pipe. This water bell evolution is described in detail in § 3.3. Throughout the change in flow rate, photographs were taken at regular intervals. These allowed the shape of the water bell surface to be extracted. The evolution of the liquid curtain under these conditions is shown in figure 16. The time interval between successive shapes is 6 s.

(ii) A new water bell was formed, also at a flow rate of 6.7 L min^{-1}. The flow rate was then steadily increased to 9.4 L min^{-1}. As the flow rate increased, so did the departure radius, and the liquid curtain crept up the central pipe. The extracted shapes for this transformation are also shown in figure 16, where the time interval is 5 s.

Using the extracted shapes, the volume of air trapped inside the bell could be calculated. Figure 16 shows that the volume remains constant so long as the curtain is not broken. The experiment was repeated using an initial flow rate of 8.9 L min^{-1}. A similar evolution of shapes was observed, and again the internal volume remained constant.

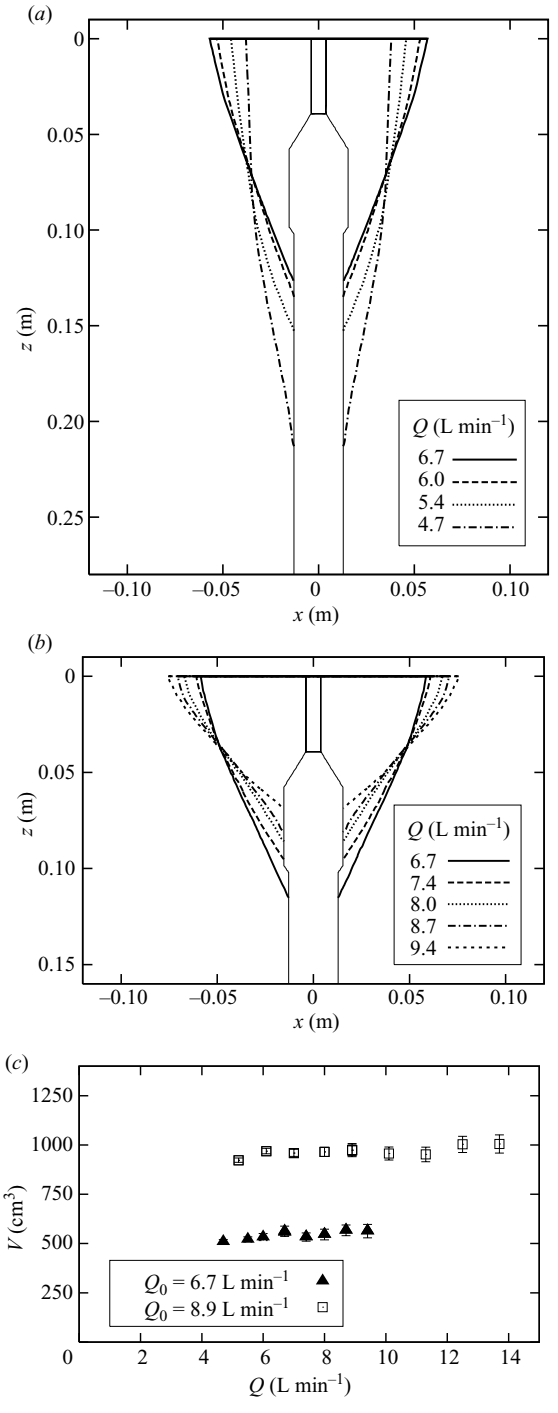

FIGURE 16. Hysteresis in water bell shape. Seventy per cent glycerol mixture with jet radius of 4 mm and Teflon surface. Bell initially formed at $Q = 6.7$ L min^{-1} and flow rate is then decreased (*a*) and increased (*b*). Internal volume of the bells is shown in (*c*), along with data for bells initially formed at $Q = 8.9$ L min^{-1}.

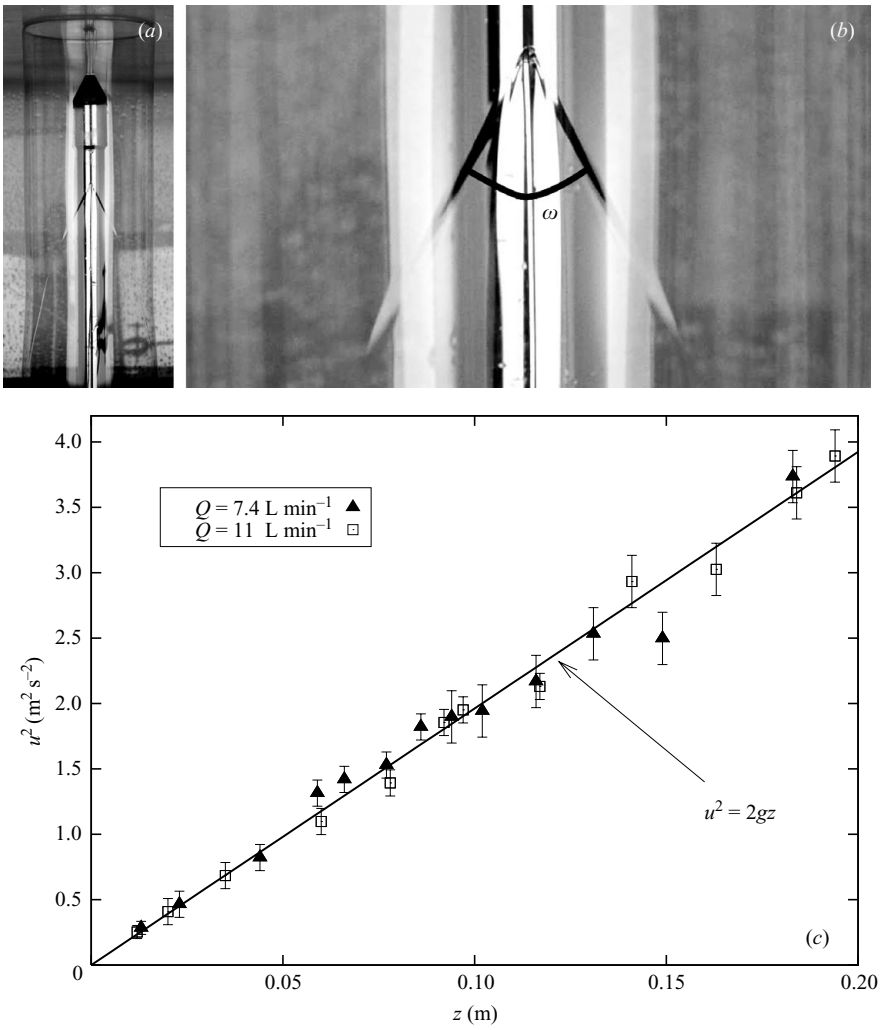

FIGURE 17. Vertical velocity of liquid in the falling film. (*a*) Cylindrical water bell. (*b*) Wake made by obstruction. (*c*) Calculated velocity, data using 70 % glycerol mixture, 4 mm jet radius and Teflon surface.

4.3. *Velocity and thickness of the falling film*

The thickness and velocity of the falling fluid were investigated using the method of Brunet *et al.* (2004). A water bell was constructed using a 70 % glycerol mixture at a flow rate of 7.4 L min^{-1}. The bell was inflated manually by blowing air through a tube to the inside of the bell. In order to simplify the measurements and calculations, the bell was enlarged until it formed a perfect cylinder. A wire of diameter 0.95 mm was used as an obstruction to the flow. The wire was placed perpendicular to the liquid film, and parallel to the view of the camera. Lights were shone on the obstruction to highlight the wake. Figure 17 shows this configuration.

The wake seemed to disappear as the wire was moved to near the top of the falling film, suggesting that these water bells are transonic, similar to those studied by Brunet *et al.* (2004). The point at which the wake disappears, or the sonic point, was too close to the solid surface for its location to be measured accurately. The

angle ω of the wake is related to the velocity of the liquid film (Taylor 1959*b*) via $u = 4\pi\gamma R/(\rho Q \sin^2(\omega/2))$, where R is the radial dimension of the cylinder. The height of the wire obstruction was varied throughout the supersonic region, and photographs were taken of the resulting wake. The angle ω was determined using Fireworks, and the average angle recorded with z (the distance below the plate). It was then possible to calculate the velocity of the liquid. The experiment was repeated using a flow rate of 11 L min^{-1}. Both sets of data lie on the same curve (see figure 17), which shows a linear relationship between u^2 and z.

The experimental measurements are well described by the curve $u^2 = 2gz$. We expect $u^2 = u_0^2 + 2gz$, and this is consistent with our results for small initial velocity u_0. It was not possible to extract any meaningful estimate of the velocity u_0 at the top of the liquid curtain, because the intercept was within the noise limits of the measurements. Knowledge of the velocity u however, allows the thickness t to be calculated using conservation of mass, $Q = 2\pi Rut$. For these cylinders, t varies as $1/\sqrt{z}$ in the supersonic region, and lies between 0.1 and 0.8 mm. The corresponding velocity varies as $\sqrt{z}$, and lies between 0.4 and 2 m s^{-1}.

5. Conclusions

In this paper we have described an unusual new class of water bells that are formed when a vertical liquid jet impinges on the underside of a plane horizontal surface. The impinging jet spreads radially outwards from the stagnation point. At a critical radius, which is determined only by the flow conditions, the liquid falls as a curtain to form a hollow bell. The shapes of the water bells displayed profound hysteresis, depending on whether the liquid flow rate was increasing or decreasing, due to the entrapped air volume. Stable bells could be formed that were closed to the atmosphere, and in which the internal pressure differed from that of the ambient. Bells could also be formed in which the internal and external pressures were the same.

The results show that the radius of departure from the plate is not heavily influenced by the path taken by the falling fluid. The departure radius is seen to increase markedly with the volumetric flow rate of the impinging jet. These experiments also show this radius has a weak inverse relationship with both the surface tension and viscosity of the fluid. The departure radius is independent of the radius of the impinging jet and the nature of the solid surface, and depends only on the volumetric flow rate. Hysteresis has an effect of less than 10 % on the value of the departure radius. When a water bell is initially formed, the departure angle ϕ, defined to be the angle made by the solid surface and the liquid sheet, is not strongly dependent on the flow rate Q. However, it is largely influenced by the history of the bell and the relationship between Q and the initial flow rate Q_0. For greatly decreasing flow rates, $Q/Q_0 \ll 1$, bell shapes such that $\phi > 90^\circ$ are possible.

The shape of the water bell is controlled by different mechanisms depending on whether or not the bell is closed to the atmosphere. Stable water bells that trap a fixed amount of air show a powerful hysteretic effect. The shape of a water bell depends on the ratio between the flow rate, and the flow rate at which the bell was initially formed, Q/Q_0. With closed water bells, if the flow rate is increased from initial formation, the top of the bell expands while the bottom contracts. When the flow rate is decreased the converse is true. In all cases, while the water bell remains stable and closed, the internal volume is constant through these transformations. The dramatic changes in the shape of the water bell appear to be due to a pressure difference across the liquid sheet, induced by the changing flow rate. The creation

of water bells open to the atmosphere at all times eliminates volume conservation and hysteresis. Theories for some of these phenomena are presented in a companion paper.

G. J. J. and C. E. J. are grateful to the Australian Research Council (ARC) for support for this work, through the Special Research Centre for Multiphase Processes at the University of Newcastle. E. C. B. and J. E. S. acknowledge funding through the Particulate Fluids Processing Centre of the ARC, and the ARC grants scheme. Thanks are due to Bob Jones, Bob Mead, John Richards, Kitty Tang and Daryl Anderson for their help with the experimental work; and to David Perry, Ashley Sneddon, Joanna Garland and Ben Dwyer for exploratory studies.

REFERENCES

Aristoff, J. M., Leblanc, J. D., Hosoi, A. E. & Bush, J. W. M. 2004 Viscous hydraulic jumps. *Phys. Fluids* **16**, S4.

Aristoff, J. M., Lieberman, C., Chan, E. & Bush, J. W. M. 2006 Water bell and sheet instabilities. *Phys. Fluids* **18**, S10.

Baird, M. H. I. & Davidson, J. F. 1962*a* Annular jets – I. Fluid dynamics. *Chem. Engng Sci.* **17**, 467–472.

Baird, M. H. I. & Davidson, J. F. 1962*b* Annular jets – II. Gas absorption. *Chem. Eng. Sci.* **17**, 473–480.

Bark, F. H., Wallin, H.-P., Gällstedt, M. G. & Kristiansson, L. P. 1979 Swirling water bells. *J. Fluid Mech.* **90**, 625–639.

Bond, W. N. 1935 The surface tension of a moving water sheet. *Proc. Phys. Soc.* B **47**, 549–558.

Boussinesq, J. 1869 Théories des expériences de Savart, sur la forme que prend une veine liquide après s'être choquée contre un plan circulaire. *C. R. Acad. Sci. Paris* **69**, 45–48.

Bremond, N. & Villermaux, E. 2006 Atomization by jet impact. *J. Fluid Mech.* **549**, 273–306.

Bridgman, P. W. 1931 *Dimensional Analysis*. Yale University Press.

Brunet, P., Clanet, C. & Limat, L. 2004 Transonic liquid bells. *Phys. Fluids* **16**, 2668–2678.

Brunet, P., Flesselles, J.-M. & Limat, L. 2001 Parity breaking in a one-dimensional pattern: a quantitative study with controlled wavelength. *Europhys. Lett.* **56**, 221–227.

Brunet, P., Flesselles, J.-M. & Limat, L. 2007 Dynamics of a circular array of liquid columns. *Eur. Phys. J.* B **55**, 297–322.

Buchwald, E. & König, H. 1936 Dynamic surface tension from liquid bells. *Ann. Physik* **26**, 661–U10.

Buckingham, R. & Bush, J. W. M. 2001 Fluid polygons. *Phys. Fluids* **13**, S10.

Bush, J. W. M., Aristoff, J. M. & Hosoi, A. E. 2006 An experimental investigation of the stability of the circular hydraulic jump. *J. Fluid Mech.* **558**, 33–52.

Bush, J. W. M. & Hasha, A. E. 2002 On the collision of laminar jets: fluid chains and fishbones. *J. Fluid Mech.* **511**, 285–310.

Button, E. C., Davidson, J. F., Jameson, G. J. & Sader, J. E. 2010 Water bells formed on the underside of a horizontal plate. Part 2. Theory. *J. Fluid Mech.* **649**, 45–68.

Clanet, C. 2000 Stability of water bells generated by jet impacts on a disk. *Phys. Rev. Lett.* **85**, 5106–5109.

Clanet, C. 2001 Dynamics and stability of water bells. *J. Fluid Mech.* **430**, 111–147.

Clanet, C. 2007 Waterbells and liquid sheets. *Annu. Rev. Fluid Mech.* **39**, 469–496.

Crapper, G. D., Dombrowski, N. & Pyott, G. A. D. 1975 Kelvin–Helmholtz wave growth on cylindrical sheets. *J. Fluid Mech.* **68**, 497–502.

Dombrowski, N. & Fraser, R. P. 1954 A photographic investigation into the disintegration of liquid sheets. *Phil. Trans. R. Soc. Lond. Ser.* A **247**, 101–130.

Dombrowski, N. & Hooper, P. C. 1964 Sprays formed by impinging jets in laminar and turbulent flow. *J. Fluid Mech.* **18**, 392–400.

Ellegaard, C., Hansen, A. E., Haaning, A., Hansen, K., Marcussen, A., Bohr, T., Hansen, J. & Watanabe, S. 1998 Creating corners in kitchen sinks. *Nature* **392**, 767–768.

Engel, O. G. 1966 Crater depth in fluid impacts. *J. Appl. Phys.* **37**, 1798–1808.

Finnicum, D. S., Weinstein, S. J. & Ruschak, K. J. 1993 The effect of applied pressure on the shape of a two-dimensional liquid curtain falling under the effect of gravity. *J. Fluid Mech.* **255**, 647–665.

Gasser, J. C. & Marty, P. 1994 Liquid sheet modelling in an electromagnetic swirl atomiser. *Eur. J. Mech.* B/*Fluids* **13**, 765–784.

Giorgiutti, F. & Limat, L. 1997 Solitary dilation waves in a circular array of liquid columns. *Physica* D **103**, 590–604.

Göring, W. 1959 Zur Abhängigkeit der Oberflächenspannung von der Bildungs – und Alterungsgeschwindigkeit der Oberfläsche. *Z. Elektrochem., Ber. Bunsenges. physik. Chem.* **63**, 1069–1077.

Hopwood, F. L. 1952 Water bells. *Proc. Phys. Soc.* B **65**, 2–5.

Huang, J. C. P. 1970 The breakup of axisymmetric liquid sheets. *J. Fluid Mech.* **43**, 305–319.

Jameson, G. J., Jenkins, C., Button, E. C. & Sader, J. E. 2008 Water bells created from below. *Phys. Fluids* **20**, 091108.

Jeandel, X. & Dumouchel, C. 1999 Influence of viscosity on the linear stability of an annular liquid sheet. *Intl J. Heat Fluid Flow* **20**, 499–506.

Lance, G. N. & Perry, R. L. 1953 Water bells. *Proc. Phys. Soc.* B **66**, 1067–1073.

Lasheras, J. C. & Hopfinger, E. J. 2000 Liquid jet atomization in a coaxial gas stream. *Annu. Rev. Fluid Mech.* **32**, 33–52.

Liu, H. 2000 *Science and Engineering of Droplets: Fundamentals and Applications*. William Andrew.

Liu, X. & Lienhard, J. 1993 The hydraulic jump in a circular jet impingement and in other thin liquid films. *Exp. Fluids* **15**, 108–116.

Magnus, H. G. 1855 Hydraulische untersuchungen. *Ann. Poggendorff* **95**, 1–59.

Mansour, A. & Chigier, N. 1990 Disintegration of liquid sheets. *Phys. Fluids* A **2**, 706–719.

Olsson, R. G. & Turkdogan, E. T. 1966 Radial spread of a liquid stream on a horizontal plate. *Nature* **211**, 813–816.

Parlange, J.-Y. 1967 A theory of water-bells. *J. Fluid Mech.* **29**, 361–372.

Pirat, C., Mathis, C., Mishra, M. & Maïssa, P. 2006 Destabilization of a viscous film flowing down in the form of a vertical cylindrical curtain. *Phys. Rev. Lett.* **97**, 184501.

Rayleigh, Lord 1914 On the theory of long waves and bores. *Proc. R. Soc.* A **90**, 324–328.

Savart, F. 1833*a* Mémoire sur la constitution des veines liquides lancees par des orifices circulaires en mince paroi. *Ann. de Chim.* **53**, 337–386.

Savart, F. 1833*b* Mémoire sur le choc de deux veines liquides animées de mouvements directement opposés. *Ann. de Chim.* **55**, 257–310.

Savart, F. 1833*c* Mémoire sur le choc d'une veine liquide lancée contre un plan circulaire. *Ann. de Chim.* **54**, 56–87.

Savart, F. 1833*d* Suite de Mémoire sur le choc d'une veine liquide lancée contre un plan circulaire. *Ann. de Chim.* **54**, 113–145.

Söderberg, L. D. & Alfredsson, P. H. 1998 Experimental and theoretical stability investigations of plane liquid jets. *Eur. J. Mech. B/Fluids* **17**, 689–737.

Squire, H. B. 1953 Investigation of the instability of a moving liquid film. *Br. J. App. Phys.* **4**, 167–169.

Taylor, G. I. 1959*a* The dynamics of thin sheets of fluid. I. Water bells. *Proc. R. Soc.* A **253**, 289–295.

Taylor, G. I. 1959*b* The dynamics of thin sheets of fluid. II. Waves on fluid sheets. *Proc. R. Soc.* A **253**, 296–312.

Thoroddsen, S. T. 2002 The ejecta sheet generated by the impact of a drop. *J. Fluid Mech.* **451**, 373–381.

Watson, E. J. 1964 The radial spread of a liquid jet over a horizontal plane. *J. Fluid Mech.* **20**, 481–499.

Wegener, P. P. & Parlange, J.-Y. 1964 Surface tension of liquids from water bell experiments. *Zeit. Phys. Chem.* **43**, 245–259.